Numerical simulation of the elastic properties of porous carbonate rocks

Henry Cao,, Austin Boyd, and Vanessa Da Silva Simoes, Schlumberger

Abstract

Three effective medium methods are used to simulate the elastic properties of porous carbonate rocks. The elastic moduli of carbonate rocks are computed for numerous models based on a set of parameters: mineral matrix, pore aspect ratio, and pore fluid content. Numerical simulations show that the bulk and shear moduli decrease with the increase of porosity. They also show that the modulus decrease is greater when the pore aspect ratio is smaller at a given porosity.

Fluid substitution is simulated using both the effective medium methods and the Biot-Gassmann equation. Consistent trends in elastic moduli are observed among these methods after fluid substitution.

The effective medium methods are also used to compute the elastic moduli of multi-type pore inclusions. The total porosity is divided into three types of different pore sizes typically observed in carbonate rocks. Both the pore aspect ratios and fluid contents can be varied with porosity types. This allows us to simulate more realistic reservoir scenarios to evaluate the effect of fluid substitution in the various porosity types observed in carbonate rocks.

Simulation comparisons from the self-consistent medium method show that pore geometry change has greater effect on elastic moduli than does pore fluid replacement. Pore geometry change has similar effects on both bulk and shear moduli. Pore fluid replacement has greater effect on the bulk modulus than on the shear modulus.

Introduction

Numerical simulation of the elastic moduli of porous carbonate rocks is very important in reservoir characterization and reservoir monitoring. A comparison of different scenarios is useful in understanding the relationships between elastic moduli and reservoir rock properties. The elastic moduli are related to seismic attributes. The reservoir rock properties include the mineral composition, porosity, pore geometry, and pore fluid content. Therefore, a simulation study can be used to unravel the links between specific seismic attributes and certain reservoir rock properties. In favorable conditions, an inversion of seismic attributes can be carried out to derive certain reservoir rock properties for exploration and production purposes.

In general, a feasibility study is carried out before a large-scale seismic survey. The feasibility is normally achieved by simulating different scenarios and determining if the desired scenarios can be resolved without ambiguity. Fluid substitution is a common technique applied in a feasibility study for both reservoir characterization and time-lapse monitoring.

In this paper, two approaches are used for fluid substitution. First, the Biot-Gassmann equation is used to link the elastic moduli of the wet rock with those of the dry rock. Next, by assuming empty-cavity porosity, effective medium methods simulate the elastic moduli of dry rock. In addition, with multi-type inclusions, effective medium methods are shown to have greater flexibility in simulating more realistic reservoir scenarios to evaluate the effect of fluid substitution in the various porosity types typically observed in carbonate rocks

Method

Three commonly used effective medium methods for carbonate rocks are the Kuster and Toksoz (KT) method (Kuster and Toksoz, 1974; Berryman, 1980), the self-consistent medium (SCM) method (Cleary et al., 1980; Berryman,1980 and 1995) and the differential effective medium (DEM) method (Norris, 1985; Zimmerman, 1991). These methods are well described by Mavko, Mukerji, and Dvorkin (2009).

A generalized form of the KT method can be represented as

$$\left(K_{KT}^{*} - K_m\right)\frac{\left(K_m - \frac{4}{3}\mu_m\right)}{\left(K_{KT}^{*} - \frac{4}{3}\mu_m\right)} = \sum_{i=1}^{N} x_i\left(K_i - K_m\right)P^{mi} \quad (1)$$

$$\left(\mu_{KT}^{*} - \mu_m\right)\frac{\left(\mu_m - \zeta_m\right)}{\left(\mu_{KT}^{*} - \zeta_m\right)} = \sum_{i=1}^{N} x_i\left(\mu_i - \mu_m\right)Q^{mi} \quad (2)$$

$$\zeta = \frac{\mu}{6}\frac{(9K+8\mu)}{(K+2\mu)}, \quad (3)$$

where the subscript m stands for the mineral matrix, K_i is the bulk modulus of the i-th inclusion, μ_i is the shear modulus of the i-th inclusion, x_i is the volume percentage of the i-th inclusion, K_{KT}^{*} is the bulk modulus of the effective medium, μ_{KT}^{*} is the shear modulus of the effective medium, and P^{mi} and Q^{mi} are the shape factors for the i-th inclusion.

Similarly, the SCM method can be represented as

$$\sum_{i=1}^{N} x_i\left(K_i - K_{SC}^{*}\right)P^{mi} = 0 \quad (4)$$

$$\sum_{i=1}^{N} x_i\left(\mu_i - \mu_{SC}^{*}\right)Q^{mi} = 0, \quad (5)$$

where K_i is the bulk modulus of the i-th inclusion, μ_i is the shear modulus of the i-th inclusion, x_i is the volume

percentage of the i-th inclusion, K_{SC}^{*} is the bulk modulus of the effective medium, μ_{SC}^{*} is the shear modulus of the effective medium, and P^{mi} and Q^{mi} are the shape factors for the i-th inclusion.

The DEM method can be represented as

$$(1-y)\frac{d}{dy}[K^{*}(y)] = (K_i - K^{*})P^{mi}(y) \qquad (6)$$

$$(1-y)\frac{d}{dy}[\mu^{*}(y)] = (\mu_i - \mu^{*})Q^{mi}(y), \qquad (7)$$

where $K^{*}(0) = K_0$ and $\mu^{*}(0) = \mu_0$ are the bulk and shear moduli, respectively, of the initial host material before adding the i-th inclusion; K_i and μ_i are the bulk and shear moduli, respectively, of the incrementally added i-th inclusion; y is the concentration of the i-th inclusion; and P^{mi} and Q^{mi} are the shape factors for the i-th inclusion.

The shape factors for several common inclusion geometries are presented in Tables 1 and 2.

Table 1: Shape Factor P^{mi} for Various Inclusions

Shape	P^{mi}
Spheres	$\dfrac{K_m + \frac{4}{3}\mu_m}{K_i + \frac{4}{3}\mu_m}$
Needles	$\dfrac{K_m + \mu_m + \frac{1}{3}\mu_i}{K_i + \frac{4}{3}\mu_m + \frac{1}{3}\mu_i}$
Disks	$\dfrac{K_m + \frac{4}{3}\mu_i}{K_i + \frac{4}{3}\mu_i}$
Penny cracks	$\dfrac{K_m + \frac{4}{3}\mu_i}{K_i + \frac{4}{3}\mu_i + \pi\alpha\beta_m}$

Table 2: Shape Factor Q^{mi} for Various Inclusions

Shape	Q^{mi}
Spheres	$\dfrac{\mu_m + \zeta_m}{\mu_i + \zeta_m}$
Needles	$\frac{1}{5}\left(\dfrac{4\mu_m}{\mu_m + \mu_i} + 2\dfrac{\mu_m + \gamma_m}{\mu_i + \gamma_m} + \dfrac{K_i + \frac{4}{3}\mu_m}{K_i + \mu_m + \frac{1}{3}\mu_i}\right)$
Disks	$\dfrac{\mu_m + \zeta_i}{\mu_i + \zeta_i}$
Penny cracks	$\frac{1}{5}\left(1 + \dfrac{8\mu_m}{4\mu_i + \pi\alpha(\mu_m + 2\beta_m)} + 2\dfrac{K_i + \frac{2}{3}(\mu_i + \mu_m)}{K_i + \frac{4}{3}\mu_i + \pi\alpha\beta_m}\right)$

Here, the following are defined as

$$\beta = \mu\frac{(3K + \mu)}{(3K + 4\mu)}$$

$$\gamma = \mu\frac{(3K + \mu)}{(3K + 7\mu)}$$

$$\zeta = \frac{\mu}{6}\frac{(9K + 8\mu)}{(K + 2\mu)}.$$

Penny cracks are used for the numerical simulations. The geometry of a penny crack is specified by the pore aspect ratio (α). The aspect ratio is defined as the ratio of the short axis versus the long axis. Figure 1 schematically shows the shape change as the pore aspect ratio varies from 0.5 to 0.01.

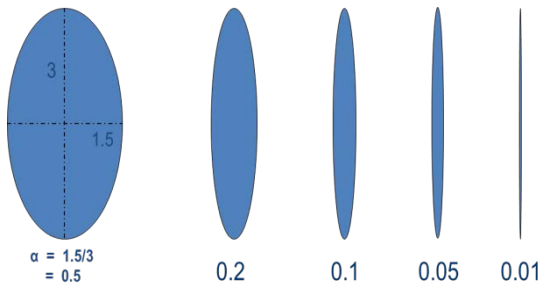

Figure 1: Shape of a penny crack pore related to the pore aspect ratio (α).

The Biot–Gassmann equation (Gassmann, 1951; Biot, 1956) provides the low-frequency relation between the elastic moduli of the saturated rock and those of the dry rock.

$$\frac{K_{sat}}{K_m - K_{sat}} = \frac{K_{dry}}{K_m - K_{dry}} + \frac{K_f}{\emptyset(K_m - K_f)} \quad (8)$$

$$\mu_{sat} = \mu_{dry}, \quad (9)$$

where K_{dry} and K_{sat} are effective bulk moduli of dry rock and saturated rock, respectively; μ_{dry} and μ_{sat} are effective shear moduli of dry rock and saturated rock, respectively; K_m is the effective bulk modulus of the composite mineral matrix; K_f is the effective bulk modulus of the pore fluid; and Ø is effective porosity.

By rearranging Eq. 8, we obtain the following explicit formulae:

$$K_{sat} = K_{dry} + \frac{\left(1 - \frac{K_{dry}}{K_m}\right)^2}{\frac{\emptyset}{K_f} + \frac{1-\emptyset}{K_m} - \frac{K_{dry}}{K_m^2}}, \quad (10)$$

and

$$K_{dry} = K_{sat} \frac{\frac{\emptyset K_m}{K_f} - \frac{K_m}{K_{sat}} + 1 - \emptyset}{\frac{\emptyset K_m}{K_f} + \frac{K_{sat}}{K_m} - 1 - \emptyset}. \quad (11)$$

A simple limestone example

For numerical simulation using the effective medium methods, the elastic properties of the host rock minerals and pore fluids are required. Table 3 lists the elastic properties of some common minerals and fluids in a typical carbonate reservoir.

Table 3: Elastic Properties of Minerals and Fluids in Typical Carbonate Reservoirs

Mineral or Fluid	Grain density (gm/cc)	Bulk modulus (GPa)	Shear modulus (GPa)
Calcite	2.7100	76.7000	32.3000
Dolomite	2.8700	94.8000	45.7000
Quartz	2.6500	38.0000	44.4000
Oil	0.8697	1.9580	0.0000
Gas	0.2884	0.0694	0.0000
Water	1.0000	2.7060	0.0000

In this simple example discussed here, the host rock consists of the mineral calcite only, and the included pores (inclusions) are fully saturated with water. For the numerical simulation, the porosity is assumed to range from 0 to 0.5. The inclusions are modeled with two aspect ratios: 0.5 and 0.01. The aspect ratio of the mineral matrix is 0.75 for SCM modeling.

Figure 2 shows the results of the numerical simulations. The results from the KT method are displayed in green, those from the SCM method are in red, and those from the DEM method are in blue.

In general, both bulk and shear moduli decrease with an increase in porosity. The decrease is greater when the aspect ratio is smaller. When the aspect ratio is large (0.5), KT simulation results are very close to SCM results. When the aspect ratio is small (0.01), KT results are significantly different from SCM results, and the KT moduli become negative when the critical porosity is exceeded. The critical porosity for the bulk modulus is different from the critical porosity for the shear modulus.

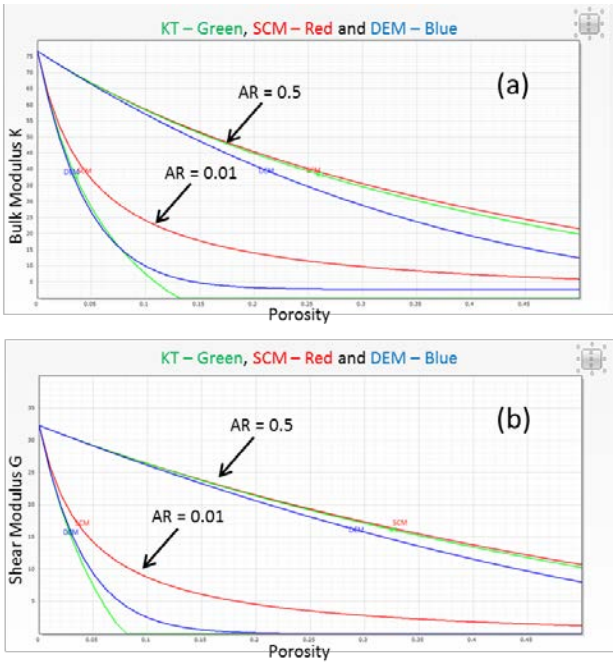

Figure 2: Effective medium simulation of water-saturated limestone with penny crack pores, showing variation of bulk modulus (a) and shear modulus (b) versus porosity. Results from two models with pores differing in aspect ratio (AR) are shown.

Fluid substitution: Effective medium methods vs Biot-Gassmann equation

The Biot–Gassmann theory is often used to obtain elastic moduli of the "dry rock" from moduli of the saturated rock, as shown in Eq. 11. When the inclusions consist of empty cavities, the effective medium methods can simulate the scenario of dry rock. The dry-rock elastic moduli derived by these two approaches are compared here.

In Figure 2, the elastic moduli of the water-saturated limestone were calculated using the three effective medium methods. By assuming empty-cavity pores in the model, we use the effective medium methods to yield the elastic moduli of the dry rock. Figure 3 displays the results of the dry-rock simulations. In general, similar trends are observed for all three methods. Therefore, for simplicity and clarity, results from the SCM method will be shown for further investigations described in this paper.

An inspection of Figs. 2 and 3 shows that the elastic moduli are reduced when the rock pores are changed from water-saturated to empty cavities at a given porosity.

The reduction increases as porosity increases. The reduction is greater when the pore aspect ratio is smaller.

The reductions in elastic moduli from the SCM method are the smallest among the three methods. The reductions in elastic moduli from the DEM method are the greatest when the aspect ratio is 0.5, whereas those from the KT method are the greatest when the aspect ratio is 0.01.

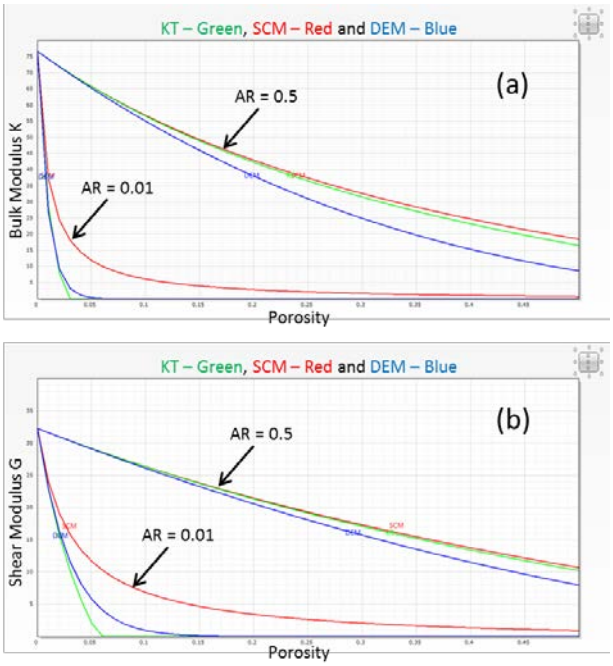

Figure 3: Effective medium simulation of dry-rock limestone with empty-cavity pores, showing variation of bulk modulus (a) and shear modulus (b) versus porosity.

Figure 4 shows the comparison between the Biot-Gassmann method and the SCM method. In this figure, the water-saturated rock elastic moduli that are calculated using the SCM method are displayed in red. The dry-rock moduli that are calculated by the Biot-Gassmann equation are displayed in green. The dry-rock moduli derived by using the SCM method and assuming empty-cavity pores are displayed in blue.

The bulk modulus dry-rock curve from the Biot-Gassmann equation coincides with the SCM dry-rock curve (Fig. 4a). As previously noted, the bulk modulus is reduced when the rock model is changed from water-saturated to dry. The reduction is greater when the aspect ratio is smaller. Larger reductions in the bulk modulus are observed for the aspect ratio of 0.01 relative to those shown for the aspect ratio of 0.5 (Fig. 4a).

In Fig. 4b, the shear modulus curve from the Biot-Gassmann approach coincides with the original curves from the SCM saturated simulation. This is expected from Eq. 9. When the aspect ratio is 0.5, the dry-rock SCM method does not produce noticeable changes in the shear modulus for the whole porosity range. When the aspect ratio is reduced to 0.01, the dry-rock SCM method yields a small reduction in the shear modulus.

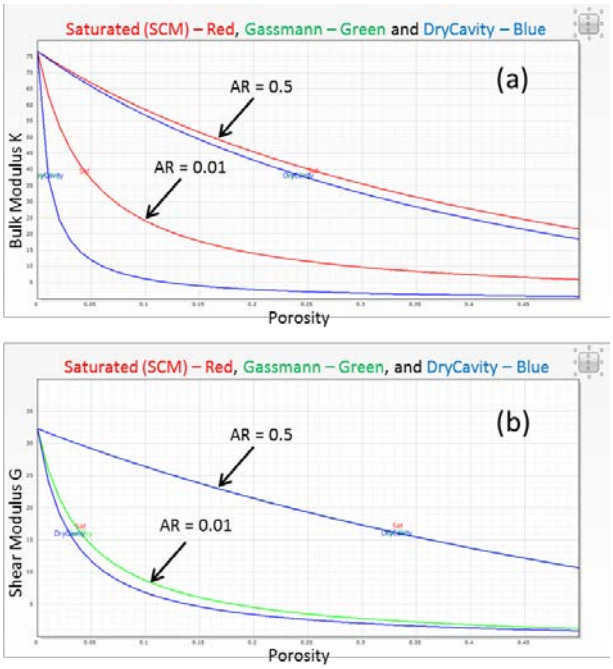

Figure 4: Variation of dry-rock limestone bulk modulus (a) and shear modulus (b) with porosity. Dry-rock data are derived from the Biot-Gassmann equation (green) and empty-cavity SCM method (blue). Saturated rock SCM data are displayed in red.

Multi-type inclusions

The size, geometry, and fluid content of the pores in a carbonate reservoir can vary significantly. In terms of pore throat size, the porosity is commonly partitioned into micro-, meso-, and macroporosity. When pore throat sizes are less than 0.5 microns, they are grouped as microporosity. When pore throat sizes are greater than 5 microns, they are grouped as macroporosity. Pores with throats sized between 0.5 and 5 microns are considered mesoporosity. For a typical carbonate reservoir, micro-, meso-, and macroporosity partitions comprise about 25%, 60%, and 15%, respectively, of the total porosity.

These porosity types have different fingerprints on common electrical wireline logs. Nuclear magnetic resonance (NMR) T2 distribution has good correspondence to pore throat size, and cutoff values can be used to interpret the porosity partitioning.

Electrical borehole images in a carbonate formation can be used to derive the vug porosity, which is an estimate of the macroporosity. However, micro- and mesoporosity cannot be distinguished from electrical images. Full waveform acoustic logs can also be interpreted for an estimate of spherical porosity. Again, micro- and mesoporosity cannot be distinguished with acoustics. Figure 5 schematically shows the porosity partitioning of a carbonate formation and the corresponding interpretations available from electrical wireline logs.

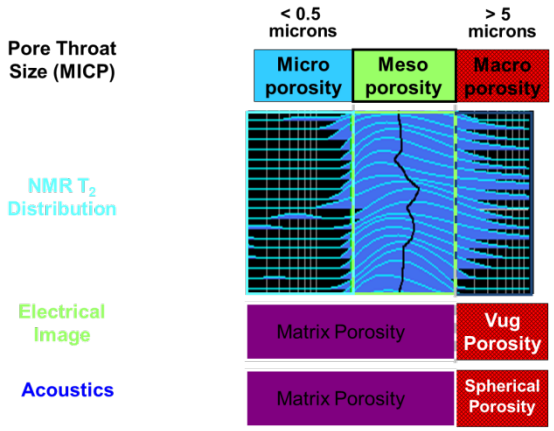

Figure 5: Schematic diagram showing the porosity partitioning of a carbonate formation.

For penny-crack inclusions, the shape factor depends on the pore aspect ratio and the elastic properties of the inclusion content. The effect of the pore aspect ratio can be investigated while the fluid contents are kept the same for all pores in the model. Vice versa, the effect of pore fluid can be investigated when the pore aspect ratios are kept the same for all pores. As shown in Table 4, two types of inclusion models are used to illustrate how elastic moduli are affected by pore geometry and pore contents, respectively. The micropores are filled with water for all models to simulate water-wet reservoirs. The wettability of carbonate rocks is controlled by the geology (Marzouk, Takezaki and Miwa, 1995). Simulation results from only the SCM method are shown here.

Table 4: List of Models Consisting of Different Pore Aspect Ratios (AR) and Pore Fluid Contents

	Microporosity		Mesoporosity		Macroporosity	
	AR	Fluid	AR	Fluid	AR	Fluid
Geometry effect	0.5	Brine	0.5	Oil	0.5	Oil
	0.01	Brine	0.5	Oil	0.5	Oil
	0.05	Brine	0.05	Oil	0.05	Oil
	0.01	Brine	0.05	Oil	0.05	Oil
Fluid effect	0.5	Brine	0.5	Oil	0.5	Oil
	0.5	Brine	0.5	Gas	0.5	Gas
	0.05	Brine	0.05	Oil	0.05	Oil
	0.05	Brine	0.05	Gas	0.05	Gas

Pore aspect ratio

The pore geometry effects on elastic moduli can be investigated by varying the pore aspect ratio of some or all pores while allowing the pore fluid content to remain the same in all pores.

Two reference models are used to show the pore geometry effect (Table 4). The aspect ratio of all three pore types for the first reference model is assumed to be 0.5. In the second reference model, the aspect ratio is assumed to be 0.05. For all models, the inclusion fluids in micro-, meso-, and macropores are brine, oil, and oil, respectively. For simplicity, only the aspect ratio of the micropores is changed to 0.01 to illustrate the pore geometry effect.

Figure 6 shows the simulation results for both reference models (AR = 0.5 and 0.05) before and after decreasing the microporosity aspect ratio to 0.01. In both scenarios, both elastic moduli decrease after the microporosity aspect ratio is decreased. The magnitude of change in the bulk and shear moduli in the first scenario is much greater than in the second scenario. The change in bulk modulus in the second scenario is less than the change in the shear modulus.

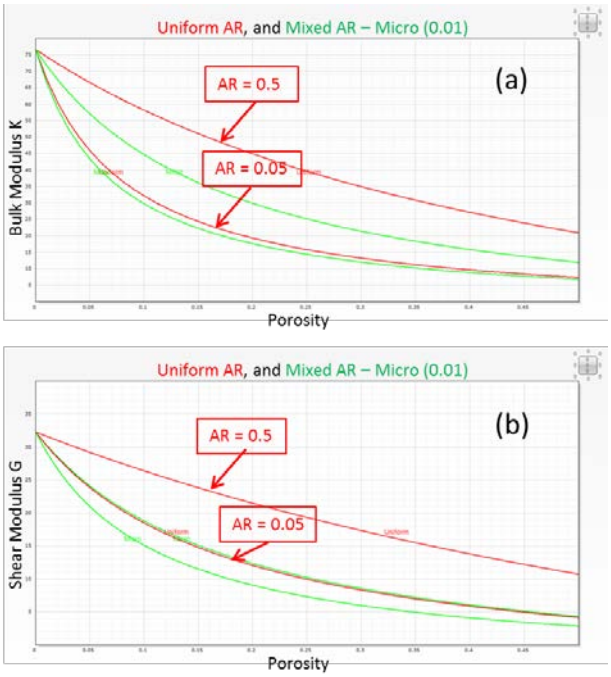

Figure 6: Pore geometry effects showing variation in bulk modulus (a) and shear modulus (b) after changing the aspect ratio of micropores. Curves in red show the elastic moduli when aspect ratios (0.5 and 0.05) are uniformly used for all pores. Curves in green show the elastic moduli after micropore aspect ratios are changed to 0.01.

Pore fluid content

Again as shown in Table 4, two reference models are used to investigate the effect of pore fluid content. For the first scenario, the aspect ratio of all three pore types is kept at 0.5. Those for the second scenario are kept at 0.05. In the reference models, the pore fluids in micro-, meso-, and macropores are brine, oil, and oil, respectively. The fluid effects are evaluated by substituting gas for oil in both meso- and macropores.

Figure 7 shows the SCM simulation results for both scenarios (AR = 0.5 and AR = 0.05) after oil is replaced by gas in meso- and macropores. In both scenarios, both elastic moduli decrease after the fluid replacement. The change in bulk and shear moduli in the first scenario is

much less than the moduli changes in the second scenario. This demonstrates that pore geometry is a significant factor when modeling fluid replacement. The pore fluid effects are greater when the pore aspect ratio is smaller. In addition, the pore fluid content has greater impact on the bulk modulus than on the shear modulus. Nevertheless, it is different from the Biot-Gassmann theory.

To summarize (Figs. 6 and 7), a change of pore geometry has a greater effect on elastic moduli than does a change of pore fluid. A pore geometry change produces similar effects to both bulk and shear moduli. A replacement of pore fluid produces a greater effect on the bulk modulus than on the shear modulus.

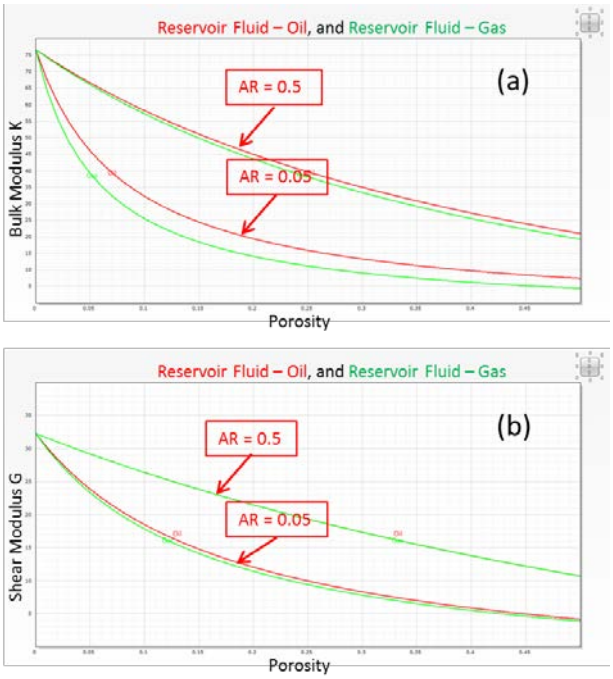

Figure 7: Pore fluid effects showing changes in bulk modulus (a) and shear modulus (b) after replacing oil in meso- and macropores with gas. Curves in red show the elastic moduli of reference models. Curves in green show the elastic moduli after the oil is replaced with gas.

Conclusions

The use of three effective medium methods to compute the elastic moduli of porous carbonate rocks when the hosting mineral matrix, porosity, pore aspect ratio, and pore fluid content are given provides insight into the relationship between rock properties and the elastic moduli. Numerical simulations show that both bulk and shear moduli decrease with the increase of porosity. They also show that the modulus reduction is greater when the pore aspect ratio is smaller at a given porosity.

Fluid substitution can be simulated using both the effective medium methods and the Biot-Gassmann equation. Consistent trends in elastic moduli changes are observed after fluid substitution using these methods.

The effective medium methods also allow computation of the elastic moduli of multi-type pore inclusions. By partitioning total porosity into three pore groups of different pore sizes typically observed in carbonates, both pore aspect ratios and fluid contents can be varied with porosity types. This allows us to simulate more realistic reservoir scenarios to evaluate the effect of fluid substitution in the various porosity types typically observed in carbonate rocks.

Comparison of simulations from the SCM method shows that change in pore geometry has a greater effect on elastic moduli than does a change of pore fluid. The pore geometry change has similar effects on both bulk and shear moduli. The pore fluid replacement has much greater effect on the bulk modulus than on the shear modulus.

References

Berryman, J.G., 1980, Long-wavelength propagation in composite elastic media: J. Acoust. Soc. Am., 68, 1809–1831.

Berryman, J.G, 1995, Mixture theories for rock properties, in T.J. Ahrens, ed., Rock Physics & Phase Relations: A Handbook of Physical Constants, AGU Ref. Shelf, vol. 3: American Geophysical Union, p. 205–228.

Biot, M.A., 1956. Theory of propagation of elastic waves in a fluid saturated porous solid. I. Low frequency range and II. Higher-frequency range. J. Acoust. Soc. Am., 28, 168–191

Cleary, M.P., I.-W. Chen, and S.-M. Lee, 1980, Self-consistent techniques for heterogeneous media: ASCE J. Eng. Mech., 106, 861–887.

Gassmann, F., 1951, Uber die elastizitat poroser medien: Vierteljahrsschrift der Naturforschenden Gesellschaft in Zurich, 96, 1–23.

Kuster, G.T., and M.N. Toksöz, 1974, Velocity and attenuation of seismic waves in two-phase media: Geophysics, 39, 587–618.

Marzouk, I., H. Takezaki, and M. Miwa, 1995, Geologic controls on wettability of carbonate reservoirs, Abu Dhabi, U.A.E., SPE 29883, presented at SPE Middle East Oil Show, Bahrain, 11–14 March.

Mavko, G., T. Mukerji, and J. Dvorkin, 2009, The Rock Physics Handbook – Tools for Seismic Analysis in Porous Media: Cambridge University Press.

Norris, A.N., 1985, A differential scheme for the effective moduli of composites: Mechanics of Materials, 4, 1–16.

Zimmerman, R.W., 1991, Elastic moduli of a solid containing spherical inclusions: Mechanics of Materials, 12, 17–24.

Acknowledgments

We would like to thank our colleagues at Schlumberger Brazil Research & Geoengineering Center, Rodolfo Oliveira, Nadege Bize, Victoria Baines, Giovanna Carneiro, Andre Souza, and Flora Marques for their support.